19 Earth Observation and Remote Sensing

Alex Damm, Dominik Brunner, Othmar Frey, Claudia Röösli, Stefan Wunderle

Swiss Commission on Remote Sensing

TALKS:

19.1 Adams J., Damm A., Irani Rahaghi A., Odermatt D., Rietze N., Schaepman-Strub G., Schaepman M., Naegeli K.: Thermal Infrared (TIR) research in Switzerland: The TRISHNA T-SEC Project

19.2 Czyż E.A., Schmid B., Hueni A., Eppinga M.B., Schuman M.C., Schneider F.D., Guillén-Escribà C., Schaepman M.E.: Multitemporal airborne reflectance spectra constrained by intraspecific genetic diversity of temperate forest

19.3 Frey O., Werner C., Caduff R.: Mobile mapping of slope stability using a dual-frequency L-/Ku-band DInSAR system configuration

19.4 Gerber L., Randin C., Milano M., Reynard E., Mariéthoz G.: NDVI Explorer – A Google Earth Engine application to visualise and extract NDVI time-series

19.5 Graf L.V Perich G., Aasen H.: EOdal: A Unified Open-Source Framework for Earth Observation Data Analysis

19.6 Gupta S., Alewell C.: Mapping soil properties at high spatial resolution using remote sensing datasets and machine learning approaches

19.7 Kesselring J., Morsdorf F., Gastellu-Etchegorry J.-P., Damm A.: Comparing the variability of abiotic parameters in structurally different forests using 3D virtual scenes and radiative transfer modelling

19.8 Mhanna S., Brunner P., Halloran L., Zwahlen., Haj Asaad.: Remote sensing based assessment of the development of Syrian refugee camps in the Orontes basin

19.9 Perich G., Turkoglu M.O., Graf L.V., Wegner J.D., Aasen H., Walter A., Liebisch F.: Pixel-based yield mapping and prediction from Sentinel-2 using spectral indices and neural networks

19.10 Portenier C., Villiger L., Wunderle S.: A deep neural network to derive cloud base height from thermal camera images

19.11 Reinders K., Verhoeven G., Sartorelli L., Manconi A.: Detection Potential of Satellite Radar Interferometry (DInSAR) over Permafrost Areas in Switzerland

19.12 Rietze N., Assmann J., Naegeli K., Damm A., Schaepman-Strub G.: Effects of drought on land surface energy fluxes in the Siberian tundra

19.13 Routh D., Röösli C.: Global-Scale Mapping and Monitoring of Land Surface Phenology: an Essential Biodiversity Variable for Conservation

19.14 Russwurm M., Pasero L., Tuia D.: Marine debris detection with noisy annotations using Sentinel-2

19.15 Sauvageat E., Hou S., Maillard Barras E., Hocke K., Haefele A., Murk A.: Diurnal ozone variability in the middle atmosphere over Switzerland observed by two microwave radiometers

19.16 Schweiger A.K., Zehnder B. & Kneubühler M.: Tree species identification using Convolutional Neural Networks and AVIRIS-NG imaging spectroscopy data

19.17 Stefko M., Bernhard P., Frey O., Hajnsek I.: Multi-seasonal observations of Great Aletsch Glacier with a multi-modal ground-based radar

19.18 Sturm J.T., Humphrey V., Santos M.J., Damm A.: Assessing the 2018 drought response of Swiss forests and its dependence on different hydrological drivers

POSTERS:

P 19.1 Goudard B., Girona T., Lupi M., Caricchi L.: Earthquake-volcano interactions at oblique subduction margins; focus on Mount Sinabung volcano (Indonesia)

P 19.2 Krochin W., Stober G., Murk A., Albers R., Plüss T.: A fully polarymetric 50 GHz temperature radiometer

P 19.3 Shiyi L., Philipp B., Irena H.: Quantitative Characterization of Glacier Surging in Karakoram using Synthetci Aperture Radar Data

P 19.4 Nguyen T.-A., Russwurm M., Kellenberger B., Tuia D.: Multi-temporal forest mapping at the Swiss alpine treeline

P 19.5 Shi G., Krochin W., Murk A., Stober G.: Ozone and Water Vapor Variability in 2019/2020 Arctic Stratospheric Polar Vortex Compared to Climatology

19.1
Thermal Infrared (TIR) research in Switzerland: The TRISHNA T-SEC Project

Jennifer Susan Adams[1], Alexander Damm[1,2], Abolfazl Irani Rahaghi[2], Daniel Odermatt[1,2], Nils Rietze[1,3], Gabriela Schaepman-Strub[3], Michael Schaepman[1], Kathrin Naegeli[1]

[1] Department of Geography, University of Zurich, Winterthurerstrasse 190, 8057 Zurich, Switzerland (jennifer-susan.adams@geo.uzh.ch)
[2] Department Surface Waters – Research and Management, Eawag, Swiss Federal Institute of Aquatic Science and Technology, Ueberlandstrasse 133, 8600 Duebendorf, Switzerland
[3] Department of Evolutionary Biology and Environmental Studies, University of Zurich, Winterthurerstrasse 190, 8057 Zurich, Switzerland

The TRISHNA (Thermal infraRed Imaging Satellite for High-resolution Natural resource Assessment) mission is a high-resolution space-time thermal infrared (TIR) mission aimed to enhance our understanding of the water cycle and improve our management of the planet's water resources (Lagouarde *et al* 2018). TRISHNA is planned for launch in 2025, and will provide global high resolution (~60 m), high revisit (3 acquisitions over 8 days) thermal remote sensing measurements. The scientific objectives of the TRISHNA mission include monitoring of terrestrial ecosystems, of the urban environment, coastal and inland waters, the cryosphere, the atmosphere, and applications to the solid Earth.

Within the TRISHNA objectives, the Swiss TRISHNA – Science and Electronics Contribution (T-SEC) project funded by ESA Prodex is comprised of a commercial part led by Syderal Swiss SA, and a scientific part led by the University of Zurich and Eawag. The scientific part of T-SEC aims to contribute towards the key TRISHNA scientific objectives, and focuses on using TIR remote sensing to understand and measure the water status and stress of continental ecosystems over mountainous and tundra regions.

This contribution aims to give an overview of the research themes addressed by T-SEC, including:

1. 3D modelling of directionality and energy balance over Swiss forests for ecosystem stress monitoring
2. Remote sensing of the surface energy budget of the alpine cryosphere
3. High resolution Lake Surface Water Temperature monitoring in Swiss perialpine and alpine lakes
4. Effect of ecosystem disturbances on land surface energy fluxes in the Siberian tundra

Priority sites in Switzerland have been identified for forests (Laegeren, Davos and Hölstein), alpine cryosphere (Murtèl/ Corvatsch, Findelengletscher, Glacier de la Plaine Morte) and hydrosphere (Lake Geneva, Ägerisee, Lej da Vadret). At a tundra reference site in the northeast Siberian Arctic was selected to investigate the use of land surface temperature for land surface energy flux and permafrost thaw research.

The four sub-projects aim to collectively improve our understanding of thermal remote sensing data and its use for monitoring water resources and energy budgets in complex ecosystems. We particularly address energy budget modelling in mountainous and boreal/tundra environments using TRISHNA measurements; gain understanding and characterise the key challenges faced by thermal remote sensing observations (e.g. directionality effects, scaling); to contribute towards TIR calibration and validation activities over selected reference sites in Switzerland (forests, cryosphere and inland waters) and tundra regions; to conduct field campaigns and collect thermal in-situ data to help quantify uncertainties of TIR measurements and products; to set up state-of-the-art reconstructions of selected sites or "virtual laboratories" allowing modelling and better understanding of thermal measurements and products; and finally investigate multi-sensor approaches and synergies with thermal remote sensing data.

REFERENCES

J.-P. Lagouarde, B.K. Bhattacharya, P. Crébassol, P. Gamet, S.S. Babu, G. Boulet *et al*. (2018) "The Indian-French Trishna Mission: Earth Observation in the Thermal Infrared with High Spatio-Temporal Resolution", *IGARSS 2018 - 2018 IEEE International Geoscience and Remote Sensing Symposium*

19.2
Multitemporal airborne reflectance spectra constrained by intraspecific genetic diversity of temperate forest

Ewa A. Czyż[1], Bernhard Schmid[1], Andreas Hueni[1], Maarten B. Eppinga[1], Meredith C. Schuman[1,2], Fabian D. Schneider[3], Carla Guillén-Escribà[1], Michael E. Schaepman[1]

[1] Department of Geography, University of Zurich, Winterthurerstrasse 190, CH-8057 Zurich, Switzerland
[2] Department of Chemistry, University of Zurich, Winterthurerstrasse 190, CH-8057 Zurich, Switzerland
[3] Jet Propulsion Laboratory, California Institute of Technology, 4800 Oak Grove Dr, Pasadena, CA 91109, USA
(ewa.czyz@geo.uzh.ch)

Remote sensing has demonstrated its potential to monitor biodiversity. It overcomes the spatial limitations of ground-based measurements and allows acquiring high –spatial, -spectral and temporal resolution data. Temporal trajectories of plants reflectance spectra hold information about dynamic of plants physiological and morphological traits. These traits and their turnover are specific for different phylogenetic groups, but vary also between individuals depending on their environment and genetic background. Higher genetic variability of populations increases its resilence to diseases and widen its evolutionary potential. Therefore, maintaining genetically variable populations, understanding drivers of genetic diversity and monitoring current stage of genetic variation is important for preventing species loss under changing environmental conditions. We propose a multitemporal approach using remote sensing data to contribute to biodiversity monitoring at the level of genetic diversity within species.

We used the imaging spectrometer APEX (Airborne Prism Experiment) to obtain a data set consisting of 27 images from 2009 – 2019 acquired across the growing seasons for the study area (Laegern, 47°28'N, 8°21'E). We compared this data set with a genetic data set consisting of microsatellite data of 68 dominant *Fagus sylvatica* L. (common beech) individuals from the site. We constructed distance matrices between individuals based on spectral data and microsatellite data to derived spectra-genetic similarities per each time of acquisition and spectral region. Further, we tested the influence of environmental variables on spectral-genetic similarities. We found that genetically similar individuals expose spectrally similar responses under higher temperatures of the day of acquisition and towards end of growing season. Based on investigated data, we will present and discuss the potential of repeated-time airborne imaging spectroscopy to assess the genetic structure of tree species at the landscape level.

19.3
Mobile mapping of slope stability using a dual-frequency L-/Ku-band DInSAR system configuration

Othmar Frey[1,2], Charles Werner[1], Rafael Caduff[1]

[1] Gamma Remote Sensing, Worbstrasse 225, CH-3073 Gümligen (frey@gamma-rs.ch)
[2] ETH Zurich, Earth Observation & Remote Sensing, Institute of Environmental Engineering, Leopold-Ruzicka-Weg 4, CH-8093 Zurich.

Recently, we have demonstrated mobile mapping of surface displacements using our in-house developed L-band interferometric synthetic aperture radar (SAR) system on a car and on a UAV (Frey et al. 2019 & 2021). Meanwhile we have consolidated our experience with repeat-pass SAR interferometry data acquisition, SAR imaging, and interferometric processing from such agile platforms and, in 2021/2022, we have started to deploy a second SAR system operating at Ku-band as part of our car-borne measurement configuration.
This new configuration permits acquiring simultaneously at L-band and at Ku-band. The Ku-band SAR system is essentially a Gamma Portable Radar Interferometer (GPRI) radar system (Werner et al. 2012, Caduff et al. 2015), yet using small horn antennas for the mobile mapping SAR mode instead of the 2m-long slotted waveguide antennas used in the regular stationary rotational real-aperture radar mode.

The dual-frequency setup is motivated by the following rationale: in steep slopes in alpine areas, which are typical objects of interest for displacement measurements and geohazard monitoring, the surface is often a mix of bare rock, debris, bare soil, and vegetation of different types and sizes. Interferometric radar measurements of these different types of land cover are variably affected by temporal decorrelation depending on the radar wavelength (see e.g. (Zebker & Villasenor 1992)). Also, different geological processes and terrain morphology leading to varying surface displacements velocities may play a role on the same mountain slope; a situation, which can be captured more accurately using different frequencies with different sensitivities towards the line-of-sight component of the displacements. In both cases frequency diversity is an advantage. Then, there are also technical aspects in the interferometric data processing, such as phase unwrapping, atmospheric path delay mitigation, and residual motion correction, for which the dual-frequency setup is beneficial.

In this work, we discuss mobile mapping of slope surface displacements from simultaneous L-band and K-band interferometric SAR measurements obtained around Innertkirchen and Guttannnen, CH. We discuss the synergies of the dual-frequency measurement configuration in terms of the sensitivity to line-of-sight displacements and temporal decorrelation in a typical measurement scenario, and we highlight its potential to better separate nuisance parameters, such as residual positioning errors of the radar sensor trajectory.

REFERENCES

Caduff, R., Schlunegger, F., Kos, A., and Wiesmann, A., 2015: “A review of terrestrial radar interferometry for measuring surface change in the geosciences,” Earth Surface Processes and Landforms, 40(2), 208–228.

Frey, O., Werner, C.L. and Coscione, R., 2019: “Car-borne and UAV-borne mobile mapping of surface displacements with a compact repeat-pass interferometric SAR system at L-band,” in Proc. IEEE Int. Geosci. Remote Sens. Symp., 274–277

Frey, O., Werner, C. L., Manconi, A., and Coscione, R., 2021: “Measurement of surface displacements with a UAV-borne/car-borne L-band DInSAR system: system performance and use cases,” in Proc. IEEE Int. Geosci. Remote Sens. Symp., 628–631.

Werner, C. L., Wiesmann, A., Strozzi, T., Kos, A., Caduff, R., and Wegmuller, U., 2012: “The GPRI multi-mode differential interferometric radar for ground-based observations,” in Proc. EUSAR 2012, 304–307.

Zebker, H. and Villasenor, J., 1992: “Decorrelation in interferometric radar echoes,” IEEE Trans. Geosci. Remote Sens., 30(5), 950–959.

19.4
NDVI Explorer – A Google Earth Engine application to visualise and extract NDVI time-series

Loïc Gerber[1], Christophe Randin[2], Marianne Milano[3], Emmanuel Reynard[3], Grégoire Mariéthoz[1]

[1] Institute of Earth Surface Dynamics (IDYST), UNIL-Mouline, Geopolis, University of Lausanne, 1015 Lausanne, Switzerland (loic.gerber.2@unil.ch)
[2] Alpine Botanical Garden Flore-Alpe, 1938 Champex-lac, Switzerland
[3] Institute of geography and sustainability (IGD), UNIL-Mouline, Géopolis, University of Lausanne, 1015 Lausanne, Switzerland

Water shortages have become common in Valais (Switzerland) during dry summers due to climate change and the resulting modification of hydrological regimes. They are expected to become more frequent and severe in the near future. Shortages in irrigation water for crops and grasslands can have serious ecological, economic, and social consequences.

We focus on the analysis of NDVI time-series for several grassland plots around the Entremont valley (Valais, CH) to better understand the relationship between irrigation and vegetation growth and to minimise the volume of water used. The goal is to identify the effects of irrigation and mows on NDVI (Gao, 1996) time-series to help inform farmers and stakeholders. All calculations and analyses were performed in Google Earth Engine (GEE) using Sentinel-2 and Planet labs images. GEE is a free and powerful cloud-based geospatial analysis platform that enables users to visualise and analyse a vast catalogue of satellite images. The rather new possibility of creating web applications directly within GEE is used in this project to bring remote sensing research to stakeholders in a straightforward manner through *NDVI Explorer*, an application we created.

Our application is now available to researchers, stakeholders and farmers involved in the project. This valuable tool allows them to visualise the NDVI (amongst other indexes) of different plots over several years whenever a cloudless image is available for both Sentinel-2 and Planet labs imagery. It is also possible to manually draw an area to be analysed directly in the application. While Sentinel-2 imagery is free and readily available in GEE, Planet imagery is not openly accessible and needs to be imported on the platform. Furthermore, *NDVI Explorer* automatically extracts time-series of the median NDVI for a predefined or user-drawn geometry over the entirety of the available images time-series, as well as median and standard-deviation maps.

Overall, the possibility of creating applications in GEE using the same programming language as the one used for regular analyses is very interesting and can be especially useful in the transmission of knowledge to stakeholders that do not have the technical or programming expertise.

REFERENCES

Gao, B. (1996). NDWI—A normalized difference water index for remote sensing of vegetation liquid water from space. Remote Sensing of Environment, 58(3), 257–266. https://doi.org/10.1016/S0034-4257(96)00067-3.

19.5
EOdal: A Unified Open-Source Framework for Earth Observation Data Analysis

Lukas Valentin Graf[1,2], Gregor Perich[1,2], Helge Aasen[1,2]

[1] Crop Science, Institue of Agricultural Science, ETH Zürich, Universitaetstrasse 2, CH-8092 Zürich (lukasvalentin.graf@usys.ethz.ch)
[2] Earth Observation and Analysis of Agroecosystems Team, Division Agroecology and Environment, Agroscope, Reckenholzstrasse 191, CH-8046 Zürich

The growing amount of Earth Observation (EO) data from satellites and in-situ measurements opens up unprecedented opportunities to study processes in the Earth system with high spatio-temporal resolution. However, to ensure that research in this area remains traceable and reproducible, a unified open-source framework for EO data management and analysis is required. Moreover, the framework should provide easy access to data and analysis for users without a background in geographic information science or remote sensing. For this reason, we developed the Earth Observation Data Analysis Library (EOdal). EOdal is entirely open-source (GPL v3.0 license) and written in Python3. This distinguishes EOdal from propietary solutions such as the Google Earth Engine (GEE). GEE is user-friendly and a powerful tool, but the underlying backend is closed-source and the use of the platform implies a tight commitment to a single service provider. This can lead to disruptions, especially in the case of an adaptation of the usage agreements.

EOdal allows working on local premises, but also supports cloud environments such as the Microsoft Planetary Computer to enable rapid scaling of EO data workflows from local to global scale. EOdal takes over large parts of the data handling, so that users can fully concentrate on their actual research questions.

Application areas of EOdal are currently in agricultural and ecophysiological research: For instance, EOdal was used to propagate radiometric uncertainties in Sentinel-2 data into land surface phenological. Further areas of application are the estimation of crop yield on the pixel level using Sentinel-2 time series and the reconstruction of crop growth dynamics from Planet Scope imagery. However, the library is by no means limited to these application areas: Its modular structure with programming interfaces makes it almost infinitely extensible and customizable.

We will explain the main concepts beyond EOdal and show-cast its capabilities. Moreover, we will summarize lessons learned and present possible further developments and our vision about a future open-source (Swiss) Earth Observation ecosystem.

19.6
Mapping soil properties at high spatial resolution using remote sensing datasets and machine learning approaches

Surya Gupta[1] and Christine Alewell[1]

[1] Department of Environmental Sciences, University of Basel, Bernoullistrasse 30, 4056 Basel, Switzerland

Spatial soil maps are essential for monitoring, management, and conservation. These maps are crucial to accessing the ecosystem services and helpful in guiding the farmers. Several global maps of soil properties are available, provided by SoilGrids (Poggio et al., 2021) and OpenLandMap (Hengl and Wheeler, 2018). However, the number of samples used and spatial resolution for these maps indicate a potentially high uncertainty and leave room for discussion. Moreover, these maps used very few samples to represent the soil properties of the whole of Switzerland. Therefore, the objective of this study was to produce soil property maps (soil organic carbon, soil texture, nitrogen, and phosphorus) for Switzerland using more data as compared to other studies (collected from the literature) with higher spatial resolution at different depths. We fitted the Quantile Random Forest (QRM) machine-learning model for spatial predictions. Each soil property was linked with environmental covariates such as topography, climate, and vegetation, which have an influence on soil properties. Each model was evaluated using five-fold spatial cross-validation. The results showed the concordance correlation coefficients (CCC) between 0.35-0.65 for predicted soil properties. To validate the resulting maps of soil properties and to compare the accuracy of the new maps with two global existing maps of soil properties such as SoilGrids and OpenLandMap, two independent datasets were used. The accuracy metrics for the new Swiss maps were considerably better than existing global maps.

REFERENCES:

Poggio, L., De Sousa, L. M., Batjes, N. H., Heuvelink, G., Kempen, B., Ribeiro, E., & Rossiter, D. (2021). SoilGrids 2.0: producing soil information for the globe with quantified spatial uncertainty. Soil, 7(1), 217-240.

Tomislav Hengl, & Ichsani Wheeler. (2018). Soil organic carbon content in x 5 g / kg at 6 standard depths (0, 10, 30, 60, 100 and 200 cm) at 250 m resolution (v0.2) [Data set]. Zenodo. https://doi.org/10.5281/zenodo.2525553

19.7
Comparing the variability of abiotic parameters in structurally different forests using 3D virtual scenes and radiative transfer modelling

Jasmin Kesselring[1], Felix Morsdorf[1], Jean-Philippe Gastellu-Etchegorry[2], Alexander Damm[1,3]

[1] Institute of Geography, University of Zurich, Winterthurerstrasse 190, CH-8057 Zürich (jasmin.kesselring@geo.uzh.ch);
[2] Centre d'Etudes Spatiales de la BIOsphère (CESBIO), Toulouse University (UPS, CNES, CNRS, IRD), 31401 Toulouse, France;
[3] Eawag, Swiss Federal Institute of Aquatic Science and Technology, 8600 Dübendorf

Vegetation releases water to the atmosphere due to transpiration, and CO_2 uptake is determined by the process of photosynthesis. The rate of this gas exchange depends on numerous biotic and abiotic variables specific to the underlying vegetation composition and ecosystem. Forest ecosystems are largely affected by water and carbon cycle dynamics, thus, studying forest gas exchange can help understanding and quantifying the consequences of climate change on these ecosystems. An established technique to estimate forest gas exchange is the use of eddy flux towers. With vertically distributed sensors, atmospheric variation of CO_2 and water vapor are measured as proxies for gas exchange on a local scale [Baldocchi, 2003]. By combining multiple eddy covariance sites, connections between regions and different ecosystems can be made. However, scaling up these local observations to a larger scale, requires several assumptions on the spatial distribution of biotic and abiotic factors. An alternative approach is available via remote sensing (RS), especially from satellites. Satellite RS for environmental monitoring has the advantage of a high spatial coverage, being non-destructive and comparable for large regions. A notable disadvantage of RS is, however, its inherent top of canopy perspective that has limited sensitivity for the vertical heterogeneity of the canopy itself [Damm et al., 2020].
This study aims to understand how common RS estimates of abiotic and biotic factors and gas exchange are related to the real 3D variability of forest ecosystems. We construct 3D virtual scenes of two contrasting forests (i.e., the mixed deciduous forest Laegern, the coniferous forest Seehornwald in Davos) using LiDAR and optical RS data. The radiative transfer model DART (Discrete Anisotropic Radiative Transfer) [Gastellu-Etchegorry et al., 2015] was used in combination with these 3D virtual scenes to simulate the abiotic factors net radiation and temperature. We then quantify the 3D distribution of these factors between both forest types and evaluate differences between the RS and the real 3D perspective.

REFERENCES

D. D. Baldocchi (2003): Assessing the eddy covariance technique for evaluating carbon dioxide exchange rates of ecosystems: Past, present and future. Global Change Biology, 9(4):479–492. A.

Damm, E. Paul-Limoges, D. Kükenbrink, C. Bachofen, and F. Morsdorf (2020): Remote sensing of forest gas exchange: Considerations derived from a tomographic perspective. Global Change Biology, 26(4): 2717–2727.

J. P. Gastellu-Etchegorry, T. Yin, N. Lauret, T. Cajgfinger, T. Gregoire, E. Grau, J. B. Feret, M. Lopes, J. Guilleux, G. Dedieu, Z. Malenovsk, B. D. Cook, D. Morton, J. Rubio, S. Durrieu, G. Cazanave, E. Martin, and T. Ristorcelli (2015): Discrete anisotropic radiative transfer (DART 5) for modeling airborne and satellite spectroradiometer and LIDAR acquisitions of natural and urban landscapes, Remote Sensing, 7(2):1667–1701.

19.8
Remote sensing based assessment of the development of Syrian refugee camps in the Orontes basin

Saeed Mhanna[1], Philip Brunner[1], Landon Halloran[1], Francois Zwahlen[1] , Ahmed Haj Asaad[2]

[1] *Centre of Hydrogeology and Geothermics, University of Neuchâtel, Neuchâtel, Switzerland (saeed.mhanna@unine.ch)*
[2] *Geo Expertise, Geneva, Switzerland*

Remote sensing is increasingly being used in the domain of humanitarian aid response, especially in areas with difficult access. Knowledge about the location and modes of expansion of refugee settlements is necessary for providing adequate aid. Because the development of these refugee settlements is often rapid and unorganized, humanitarian organizations often fall short in responding to the needs of their inhabitants. Moreover, uncontrolled expansions might place refugees at an elevated risk with respect to natural disasters (e.g., floods, storms and wildfires).

The ongoing armed conflict in Syria has so far resulted in 5.6 million refugees, mostly hosted in Turkey (65.1%) and Lebanon (14.8%) (UNHCR, 2022), as well as 6.7 million living in internal displacement (IDMC, 2021). In this study, we use satellite imagery and machine learning to produce yearly Landuse/Landcover (LU/LC) maps to track changes due to the conflict within the Orontes river basin, which extends across Lebanon, Syria and Turkey. Landsat 5, 7 and 8 datasets were selected spanning from 2004 to 2021 and processed using the cloud computing platform Google Earth Engine. Training/validation data points were collected from high resolution imagery and were used to train a Random Forest classifier to classify the yearly image composites. These maps allowed us to distinguish three different types of refugee camps/settlements. In Syria, Internally Displaced People (IDP) camps are characterized by a high degree of randomness and a significant sharp increase after 2019 (Figure 1). In Lebanon, refugees settled in the outskirts of major cities and peri-urban expansion commenced after the beginning of the war in 2011. Finally, highly organized camp cites were constructed in Turkey and informal settlements were restricted. The results of this study can be used to better manage the water resources for the refugees and IDPs within the Orontes river basin, in addition to monitoring and managing the expansion of these settlements.

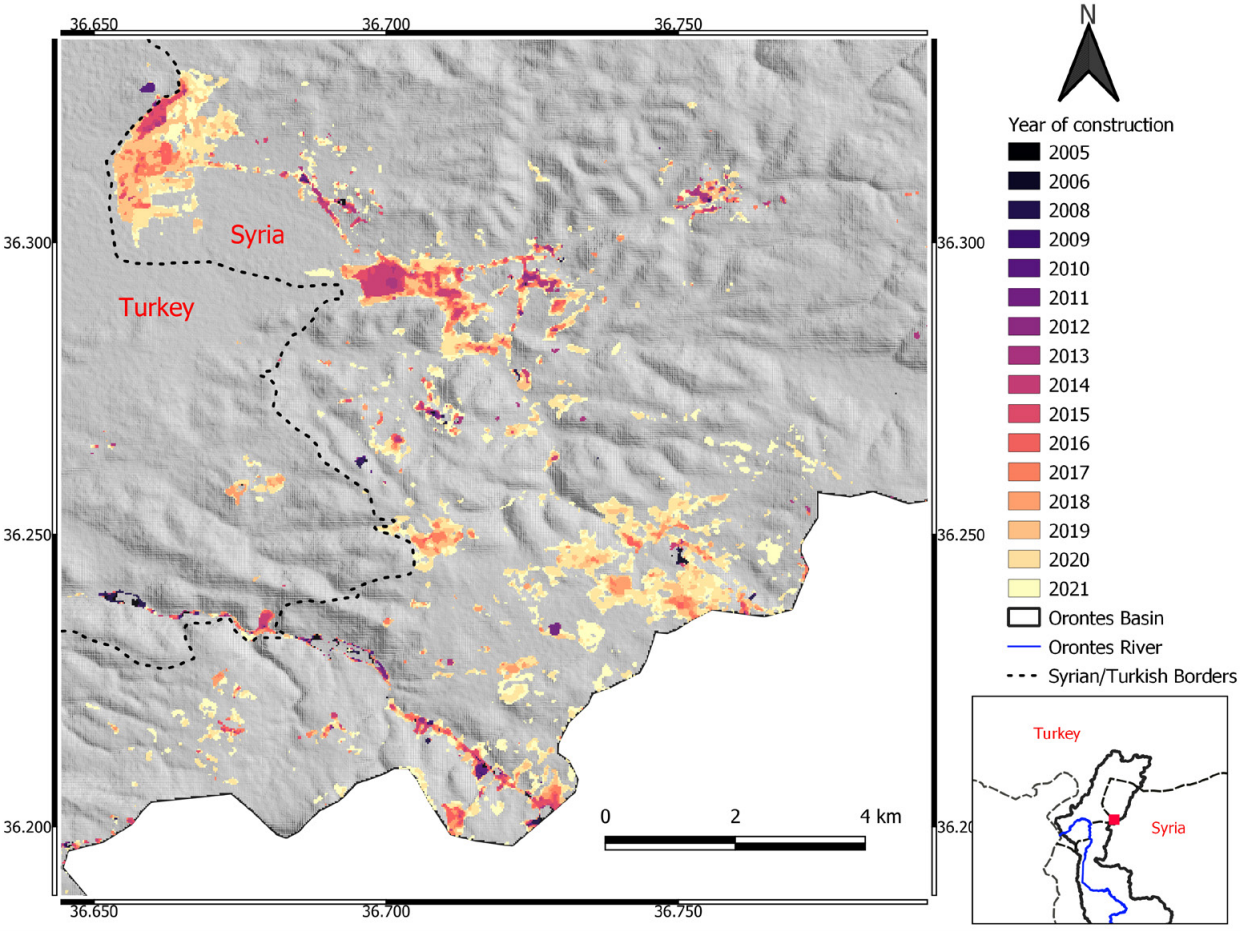

Figure 1. Yearly expansion of the IDP camps on the Syria/Turkish borders from 2005 to 2021.

REFERENCES

IDMC. (2021, December). Total Number of IDPs. Retrieved from https://www.internal-displacement.org/countries/syria.
UNHCR. (2022, July). Total Registered Syrian Refugees. Retrieved from data.unhcr.org.

19.9
Pixel-based yield mapping and prediction from Sentinel-2 using spectral indices and neural networks

Gregor Perich[1], Mehmet Ozgur Turkoglu[2], Lukas Valentin Graf[1,3], Jan Dirk Wegner[2,4], Helge Aasen[1,3], Achim Walter[1], Frank Liebisch[5]

[1] Crop Science, ETH Zurich
[2] EcoVision Lab, Photogrammetry and Remote Sensing, ETH Zurich
[3] Remote Sensing Team, Agroecology and Environment, Agroscope
[4] Institute for Computational Science, University of Zurich
[5] Agroecology and Environment, Agroscope

Mapping and predicting crop yield on a large scale is increasingly important for use cases such as policy-making, risk insurance and precision agriculture applications at farm and field scale. These have the potential to better manage agro-ecosystems, therefore help reduce the environmental impact of agriculture. The higher spatial resolution of Sentinel-2 compared to Landsat allows for satellite-based crop yield mapping even in relatively small scaled agricultural settings such as found in Switzerland and other central European regions. In this study, five years (2017-2021) of cereal crop yield data from a combine harvester were used to model crop yield on a spatial scale corresponding to the Sentinel-2 pixel level. Three established methods from literature using i-ii) spectral indices and iii) raw satellite reflectance as well as iv) a recurrent neural network (RNN) were chosen for analysis. Although the RNN approach did not outperform the other methods, it was more efficient because of the comparatively simple end-to-end training of the model, resulting in much less time spent on data cleaning and feature extraction needed for spectral index time series analysis. The RNN was also able to discriminate cloudy data by itself, reaching similar performance levels as if using pre-processed, cloud-free data. Modelling was performed on individual years, all years combined and on unseen years using leave-one-year-out cross-validation. The models performed best when using data from all years (R^2 up to 0.88, relative RMSE up to 10.49%) and showed poor performance when predicting on unseen data years, especially for years with previously unknown weather patterns. This highlights the importance of yearly model calibration and the need for continuous data collection enabling long time series for future crop yield models.

19.10
A deep neural network to derive cloud base height from thermal camera images

Céline Portenier[1], Leonie Villiger[2], Stefan Wunderle[1]

[1] Oeschger Centre for Climate Change Research and Institute of Geography, University of Bern (celine.portenier@giub.unibe.ch)
[2] Institute for Atmospheric and Climate Science, ETH Zurich

Observing atmospheric conditions such as the height of a cloud ceiling is extremely important for air traffic management. Instruments to accurately measure the cloud`s base height from the ground (so-called Ceilometers) are extremely expensive and are limited to point measurements vertically oriented to the atmosphere. An alternative solution are upward facing thermal cameras. The temperatures measured by such cameras decrease significantly if a cloud is present; the higher the cloud, the lower the measured temperature. However, the thermal camera does not correct for the atmospheric water vapour between the ground and the measured cloud. Thus, the relation between the measured temperature and the cloud base height is complex, but can be learned by a deep neural network (DNN). In our study, we propose to use parallel measurements of a Ceilometer, a thermal camera, and measurements of meteorological variables (surface pressure, relative humidity, and air temperature) as an input for a DNN to predict the cloud base height from temperatures measured by the thermal camera. We present different approaches using deep classification, deep regression, and a convolutional neural network and illustrate how the trained networks predict cloud base height compared to the nearby Ceilometer measurements. Finally, we use a hemispherical webcam to analyze different cloud types in relation to the predicted cloud base height information.

19.11
Detection Potential of Satellite Radar Interferometry (DInSAR) over Permafrost Areas in Switzerland

Kristina Reinders[1], Govert Verhoeven, Luca Sartorelli[2], Andrea Manconi[3]

[1] *Delft University of Technology, Stevinweg 1, NL-2628 CN Delft, The Netherlands (k.j.reinders@tudelft.nl)*
[2] *SkyGeo, Oude Delft 175, NL-2611 HB Delft, The Netherlands*
[3] *WSL Institute for Snow and Avalanche Research SLF, Flüelastrasse 11, CH-7260 Davos*

Glaciers and permafrost declined during the last decade and are expected to continue with this trend in almost all regions throughout the 21st century (Hock et al., 2019). This will increase the natural hazard potential in alpine regions (Hock et al., 2019; Gobiet et al., 2014; Probst et al., 2013). This year, glacier collapses in the Grand Combin and the Marmolada have already caused several fatalities (SRF, 2022).

Monitoring the alpine permafrost is therefore crucial to asses the vulnerability of structures in these areas and plan countermeasures. Currently, the most common method to monitor permafrost is with temperature and displacement measurements in boreholes. However drilling boreholes and monitoring temperature in high alpine environment is not trivial. In addition, the information is limited at few points and might be not representative of the spatial variabilities. For this reason, remote sensing can provide valuable solutions. For example, one method to monitor displacements over large areas is differential interferometry on spaceborne synthetic aperture radar (DInSAR) (Hanssen, 2001). However, this technique is still rarely used in common practice to monitor permafrost areas. This is due to several limitations in terms of spatial and temporal resolutions, as well as intrinsic limitations of DInSAR over high alpine areas. The advent of new modern satellite missions such as the ESA Copernicus Sentinel-1 provides new opportunities to perform systematic investigations and build monitoring programs at regional scales.

In this work, we explored the detection potential of permafrost areas in the Swiss alps with DInSAR. We use Sentinel-1 data acquired over Switzerland spanning 5 orbits (descending tracks 136, 66, 168 and ascending tracks 88 and 15) the digital elevation model Copernicus 30 m, and the permafrost indication map provided by of the Swiss Institute for Snow and Avalanche Research (SLF, 2019), to determine the theoretical detection potential and visibility of the areas of interest. We calculated the R-index, accoring to Notti et al. (2014) for entire Switzerland and then focused on only the permafrost areas. Fig. 1 shows an example of R-Index maps produced for the two ascending tracks. Secondly we analyzed the results of Persisten Scatterer Interferometry (PSI) obtained over the Canton Wallis to assess into details the real results over selected places of interest. Our results will help understanding if displacements in permafrost areas can be detected efficiently and monitored, and if this approach can be used to optimise mitigation strategies in high alpine areas.

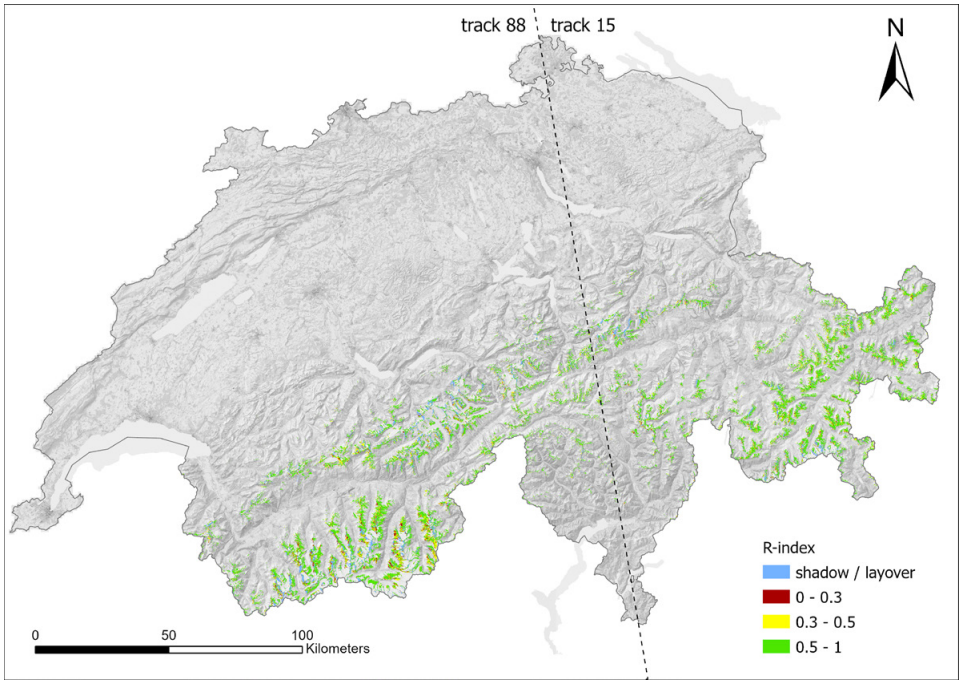

Figure 1. R-index for ascending tracks in permafrost areas, where red means the visibility of the area may not be good and green means that the area has a good visibility.

REFERENCES

Gobiet, A., Kotlarski, S., Beniston, M., Heinrich, G., Rajczak, J., and Stoffel, M. 2014: 21st century climate change in the European Alps—A review, Science of The Total Environment, 493, 1138–1151

Hanssen, R. F. 2001: Radar Interferometry: Data Interpretation and Error Analysis, Kluwer Academic Publishers, Dordrecht

Hock, R., Rasul, G., Adler, C., Cáceres, B., Gruber, S., Hirabayashi, Y., Jackson, M., Kääb, A., Kang, S., Kutuzov, S., et al. 2019: High Mountain areas

Notti, D., Herrera, G., Bianchini, S., Meisina, C., García-Davalillo, J. C., and Zucca, F. 2014: A methodology for improving landslide PSI data analysis, International Journal of Remote Sensing, 35, 2186–2214

Probst, T., Wicki, W., Zischg, A., and Pichler, A. 2013: Alpine strategy for adaptation to climate change in the field of natural hazards

SRF, Zwei Tote nach Eissturz im Wallis, May 27, 2022, https://www.srf.ch/news/schweiz/abgebrochene-eisbrocken-zwei-tote-nach-eissturz-im-wallis

SRF, gletscherabbruch-in-italien-fordert-tote, July 3, 2022, https://www.srf.ch/play/tv/tagesschau/video/gletscherabbruch-in-italien-fordert-tote?urn=urn:srf:video:98cbc087-36ac-4637-a2d1-9dc8047a6a57

Swiss institute of snow and avalanche research, 2019: neue Permafrost- und Bodeneiskarte des SLF (PGIM), https://www.slf.ch/pgim

19.12
Effects of drought on land surface energy fluxes in the Siberian tundra

Nils Rietze [1], Jakob Assmann [1], Kathrin Naegeli [2], Alexander Damm [2,3], Gabriela Schaepman-Strub [1]

[1] Spatial Ecology and Remote Sensing, Department of Evolutionary Biology and Environmental Sciences, University of Zurich, Winterthurerstr. 190, CH-8057 Zürich (nils.rietze@uzh.ch)
[2] Remote Sensing Laboratories, Department of Geography, University of Zurich, Winterthurerstr. 190, CH-8057 Zürich
[3] Remote Sensing of Water Systems, Department of Geography, University of Zurich, Winterthurerstr. 190, CH-8057 Zürich

The rapidly warming climate and associated changes, such as plant community shifts, droughts and wildfires, alter land surface energy fluxes in the Arctic tundra. Droughts and shifts in plant community composition might modify latent and sensible heat fluxes, resulting in altered land surface feedbacks to the regional climate.
Our study aims to analyse drivers of plant thermoregulation (the vegetation‘s ability to cool its canopy by evapotranspiration) combining remotely sensed estimates of heat fluxes and in situ data of microclimate. We collected drone-based optical and thermal imagery during peak growth season (July-August) of a very dry summer (2020) and a hydrologically average summer (2021) in the Kytalyk national reserve in north-eastern Siberia (70.83° N, 147.49° E).
Additionally, we measured biotic, soil and atmospheric variables, including species composition, soil temperature and moisture, precipitation, and air temperature. We first quantified the drivers of micro-scale thermoregulation across different plant communities, and then investigated the effects of summer drought on thermoregulation.
During both years, plant community types differed in their thermoregulation. Communities associated with moist soils had the strongest cooling of the canopy, whereas drier plant communities showed weaker thermoregulation or a complete lack thereof. Thermoregulation was weaker in the summer with drought (2020) across all vegetation types, indicating that the plants experience water limitation during drought conditions at the research site.
Overall, our study highlights the importance of considering plant community composition and drought conditions when estimating landscape energy fluxes in the Arctic tundra. Further work is needed to quantify the contributions of both factors to regional climate feedbacks across the Arctic tundra.

19.13
Global-Scale Mapping and Monitoring of Land Surface Phenology: an Essential Biodiversity Variable for Conservation

Devin Routh[1,2], Claudia Röösli[2]

[1] *S[3]IT: Service and Support for Science IT; University of Zürich, Winterthurerstrasse 190, CH 8057 Zürich*
[2] *Remote Sensing Laboratories, Department of Geography; University of Zürich, Winterthurerstrasse 190, CH 8057 Zürich*

Keywords: remote sensing, land surface phenology, conservation, monitoring, biodiversity, big data

Human society has placed enormous stress on ecosystems across the globe, with one of the many consequences being the loss of biodiversity (Johnson et al., 2017; Habibullah et al., 2022). Conservation efforts, however, can lessen these environmental stressors and mitigate some of the damage. As a direct response to initiatives aiming to reduce biodiversity loss, the Group on Earth Observations - Biodiversity Observation Network (GEO BON) has proposed a common framework of essential biodiversity variables (EBVs) to implement global-scale monitoring of several biodiversity metrics following the concept of the Essential Climate Variables (ECVs)(Bojinski et al., 2014). One contribution to the framework of these EBVs is Land Surface Phenology (LSP), which is the study of vegetation seasonal activity at the ecosystem scale (Schwartz, 2013). In response, our group has developed an algorithm to determine LSP metrics that uses remotely sensed satellite imagery to create global maps that will allow such ecosystem monitoring at a previously impractical scale. Using the Normalized Difference Vegetation Index (NDVI) time-series data from high resolution satellite imagery (i.e., based mainly on Sentinel-2 at 10m resolution), the algorithm harnesses state-of-the-art statistical methods to generate “seasonal curves” at every valid pixel location that will allow end-users and conservationists to study various plant growing season metrics such as start-of-season, end-of-season, length-of-season, etc. Because the algorithm is being implemented on Google Earth Engine, a planetary scale remote sensing and Geographic Information System (GIS) platform, it will be possible to generate these maps globally on both data from past years as well as on future data that is being continuously collected (Gorelick et al., 2017). Thus, generating new yearly maps will be both possible and efficiently achieved to support ongoing conservation monitoring efforts.

In this session we will present an overview of the methods that have been used in the project, the challenges that have been encountered, and an outlook of the upcoming work. As such, specific topics will include: (1) the statistical process used to create the “seasonal curves”, which is an algorithm called Differential Evolution Optimization that was chosen due to a variety of advantages including its functional flexibility and the straight-forward array mathematics used in its calculations (Mullen et al., 2011); (2) the application of the LSP algorithm at a global-scale involves deliberate planning and development on the Google Earth Engine platform to accommodate all ecosystem types (e.g., boreal forest, temperate forest, mediterranean scrubland, etc.) within a single framework; (3) the ultimate goal is the creation of a publically available mapping portal that allows users to explore the outputs as they are available year-by-year.

REFERENCES

Bojinski, S., Verstraete, M., Peterson, T. C., Richter, C., Simmons, A., & Zemp, M. (2014). The Concept of Essential Climate Variables in Support of Climate Research, Applications, and Policy. Bulletin of the American Meteorological Society, 95(9), 1431–1443. https://doi.org/doi:10.1175/BAMS-D-13-00047.1

Gorelick, N., Hancher, M., Dixon, M., Ilyushchenko, S., Thau, D., & Moore, R. (2017). Google Earth Engine: Planetary-scale geospatial analysis for everyone. Remote sensing of Environment, 202, 18-27. https://doi.org/10.1016/j.rse.2017.06.031

Habibullah, .S., Din, B.H., Tan, SH. et al. Impact of climate change on biodiversity loss: global evidence. Environ Sci Pollut Res 29, 1073–1086 (2022). https://doi.org/10.1007/s11356-021-15702-8

Johnson, C. N., Balmford, A., Brook, B. W., Buettel, J. C., Galetti, M., Guangchun, L., & Wilmshurst, J. M. (2017). Biodiversity losses and conservation responses in the Anthropocene. Science, 356(6335), 270 LP – 275. https://doi.org/10.1126/science.aam9317

Mullen, K., Ardia, D., Gil, D., Windover, D., Cline, J. (2011). DEoptim: An R package for global optimization by Differential Evolution. Journal of Statistical Software, 40(6), 1-26. https://doi.org//10.18637/jss.v040.i06

Schwartz, M. D. (2013). Phenology: An Integrative Environmental Science. In M. D. Schwartz (Ed.), Phenology: An Integrative Environmental Science (Vol. 9789400769). Springer Netherlands. https://doi.org/10.1007/978-94-007-6925-0

19.14
Marine debris detection with noisy annotations using Sentinel-2

Marc Russwurm, Laura Pasero, Devis Tuia

Environmental Computer Science and Earth Observation Laboratory (ECEO), École Polytechnique Fédérale de Lausanne, Rue de IIndustrie 17, CH-1950-Sion (marc.russwurm@epfl.ch)

Marine Litter is a growing ecologic concern that needs to be addressed on a global scale. While satellite and meteorological data is abundant, few advances have been made toward continuously monitoring marine litter aggregated in floating patches on the oceans. As detecting individual objects is infeasible with current satellite resolutions, researchers resort to windrows as a proxy for marine litter (Arias et al., 2021). These windrows form lines of aggregated floating debris that often contain plastic litter at a sizeable fraction depending on the geographic region.

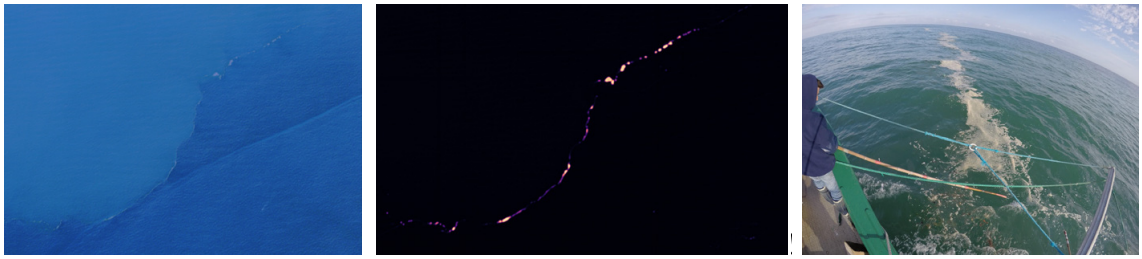

Figure 1. A Sentinel-2 image near Accra, Ghana, showing RGB representation of floating marine debris (left) alongside model predictions of Mifdal & Rußwurm (2021), which serves as a baseline for the detection module developed within ADOPT (center). The right image is by Ruiz et al. (2020), who studied the feasibility of collecting litter within these windrows on ship-based platforms at the Bay of Biscay, France.

In this work, we train a deep learning segmentation model (U-Net) to identify patches of floating marine debris that are detectable with Sentinel-2 resolution and serve as a proxy for marine litter. Figure 1 illustrates this problem with one example Sentinel-2 satellite image (left) and model predictions (Mifdal & Russwurm, 2021) (center). The shown line is a windrow similar to the image on the right of Ruiz et al., (2020), who proposed using these rows for efficient clean-up of marine litter that is often aggregated in windrows.

Label noise is a major challenge for this application. Marine debris is inherently difficult to annotate due to unclear boundaries and a permanent mixture with water. Additionally, labels are often coarse and simplified, as shown in Figure 2, where the original line-based hand annotations are displayed in the center column. These annotations roughly follow the shape of the marine debris but do not always capture the actual geometric shape. This leads to label noise in the available annotations, which provides a contradictory learning signal for the model. We address the noisy annotations by testing an automated refinement heuristic that clusters pixels in the local spatial neighborhood around an annotated debris into two classes: one for the debris itself and one for water as the background. The result of this heuristic is shown in the right column of Figure 2. We evaluated the approach experimentally in a hold-out region (near Lagos, Nigeria) and found that the model predictions improved substantially with our label refinement approach.

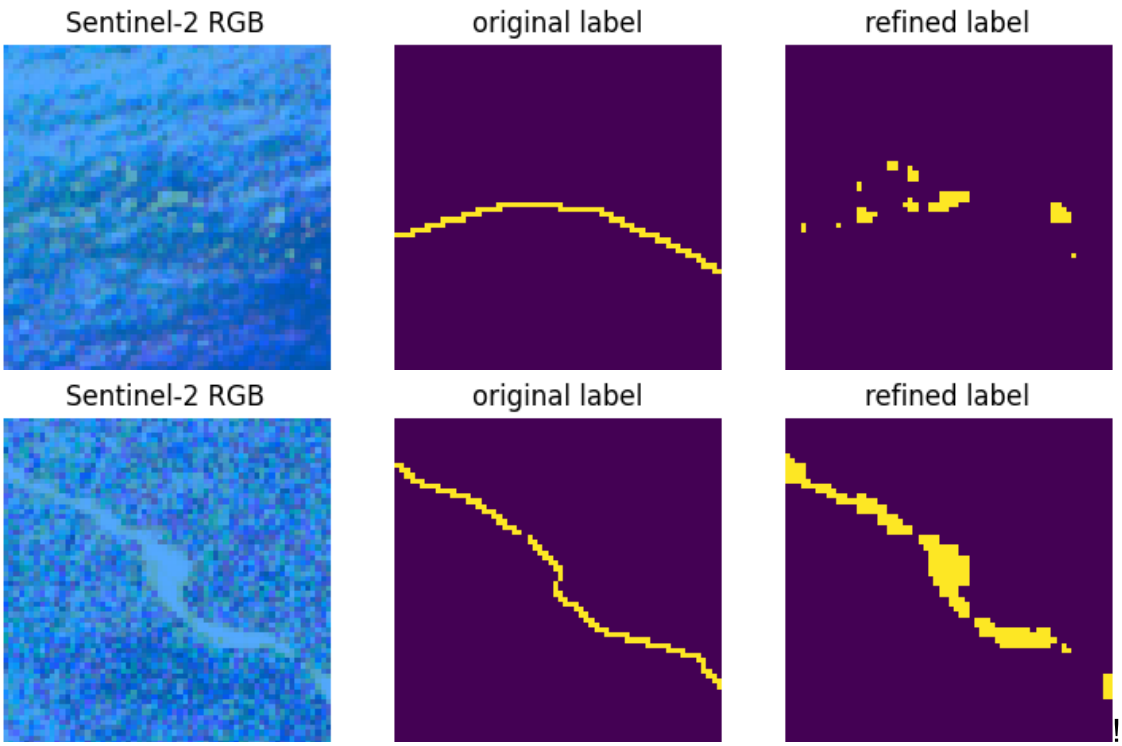

Figure 2. Two examples of the label refinement heuristic. In Mifdal & Russwurm (2021), rough annotations have been made by drawing lines. This does not always represent the true nature of objects shown in the images. The refinement algorithm clusters pixels by their similarity, leading to more realistic annotations (right).

REFERENCES

Arias, M., Sumerot, R., Delaney, J., Coulibaly, F., Cozar, A., Aliani, S., Suaria, G., Papadopoulou T., Corradi, P. & Corradi, P. (2021, July). Advances on Remote Sensing of Windrows as Proxies for Marine Litter Based on Sentinel-2/MSI Datasets. In 2021 IEEE International Geoscience and Remote Sensing Symposium IGARSS (pp. 1126-1129). IEEE.

Mifdal, J., Longépé, N., and Rußwurm, M.: Towards detecting floating objects on a global scale with spatial features using Sentinel-2, ISPRS Ann. Photogramm. Remote Sens. Spatial Inf. Sci., V-3-2021, 285–293, https://doi.org/10.5194/isprs-annals-V-3-2021-285-2021, 2021.

Ruiz, I., Basurko, O. C., Rubio, A., Delpey, M., Granado, I., Declerck, A., Mader, J. and Cózar-Cabañas, A. (2020). Litter windrows in the south-east coast of the Bay of Biscay: an ocean process enabling effective active fishing for litter. Frontiers in Marine Science. 7, 308.

19.15
Diurnal ozone variability in the middle atmosphere over Switzerland observed by two microwave radiometers

Eric Sauvageat[1,2], Shengyi Hou[1], Eliane Maillard Barras[3], Klemens Hocke[1,2], Alexander Haefele[3], Axel Murk[1,2]

[1] *Institute of Applied Physics, University of Bern, Sidlerstrasse 5, CH-3012 Bern (eric.sauvageat@unibe.ch)*
[2] *Oeschger Centre for Climate Change Research, University of Bern, Hochschulstrasse 4, CH-3012 Bern*
[3] *Office Fédéral de Météorologie et de Climatologie MétéoSuisse, Chemin de l'Aérologie 1, CH-1530 Payerne*

Microwave radiometers can measure ozone profiles in the middle atmosphere (~20-75 km) over a large range of atmospheric conditions. Unlike many other remote sensing techniques, they are able to provide the high temporal resolution and continuous sampling required for a comprehensive study of ozone diurnal variability. In Switzerland, two ozone radiometers are operated in the vicinity of each other (40 km) since over 20 years in Payerne (MeteoSwiss) and in Bern (Institute of Applied Physics). Recently, their calibration and retrieval algorithms have been fully harmonized and updated time series are now available since 2010, showing significant improvements compared to the old time series (Sauvageat, 2022).

Using the harmonized ozone time series, we investigate the strato-mesospheric ozone diurnal cycle derived from these two instruments, in particular its seasonal and interannual variability over the last decade. We find a good agreement between the two radiometers and perform cross-validation study against various other datasets. First, we compare it with a climatology based on the Goddard Earth Observing System (GEOS-5) general circulation model. Second we use a set of free-running simulations from the Whole Atmosphere Community Climate Model (WACCM). Finally, we show first evidence of short-term diurnal cycle variability that can be detected in the radiometer time series.

REFERENCES

Sauvageat, E., Maillard Barras, E., Hocke, K., Haefele, A., and Murk, A.: Harmonized retrieval of middle atmospheric ozone from two microwave radiometers in Switzerland, Atmos. Meas. Tech. Discuss. [preprint], https://doi.org/10.5194/amt-2022-212, in review, 2022.

19.16
Tree species identification using Convolutional Neural Networks and AVIRIS-NG imaging spectroscopy data

Anna K. Schweiger[1], Benjamin Zehnder[1], Mathias Kneubühler[1]

[1] Remote Sensing Laboratories, Department of Geography, University of Zurich, Winterthurerstrasse 190, CH-8057 Zürich (anna.schweiger@geo.uzh.ch)

Tree species identification is important for biodiversity and ecosystem service assessments, carbon stock modeling and forest management. A Convolutional Neural Network (CNN) is a powerful type of Deep Learning that incorporates object context to identify objects within images. However, the general perception is that CNNs are relatively data-hungry, meaning that hundreds to thousands of training samples are needed to achieve reasonable predictive accuracy. Here we show that CNNs can be effectively trained for the identification of five common tree species based on only around 60 samples per species by using particularly information-rich remote sensing data, namely spectral imagery.

We conducted our study in Jurapark Aargau, a Swiss regional park of national importance. Our aim was to train a CNN for the identification of the five most common tree species in the area, which are beech (*Fagus sylvatica* L.), oak (*Quercus robur* L.), ash (*Fraxinus excelsior* L.), linden (*Tilia platyphyllos* Scop.) and red pine (*Pinus sylvestris* L.), based on AVIRIS-NG airborne imaging spectroscopy data. AVIRIS-NG collects spectral data in 431 bands covering the 380 nm to 2510 nm wavelength range with a mean spectral sampling interval of 5 nm and a spatial resolution of around 2 m on the ground. We collected tree identity and coordinate information of 331 trees in total. We matched tree positions to the airborne imagery using an individual tree crown delineation algorithm applied to the SwissSURFACE3D LiDAR (Light Detection and Ranging) product provided by Swisstopo. We reduced the AVIRIS-NG data to the main axes of spectral variation and augmented the tree crown images used for training the CNN by adding random noise, changing brightness and rotation. Our CNN correctly identified over 70% of all tree species and performed overall better than other classifiers, including Random Forest and Support-Vector Machine. Our study indicates that the high data demand of Deep Learning Algorithms may be counterbalanced by the information-richness of the data. We suggest further testing of this hypothesis through sensor integration, for example by including data collected by multispectral, LiDAR, thermal and SAR (Synthetic Aperture Radar) sensors.

19.17
Multi-seasonal observations of Great Aletsch Glacier with a multi-modal ground-based radar

Marcel Stefko[1], Philipp Bernhard[1], Othmar Frey[1], Irena Hajnsek[1]

[1] *Chair of Earth Observation and Remote Sensing, ETH Zurich, Leopold-Ruzicka-Weg 4, CH-8093 Zurich (stefko@ifu.baug.ethz.ch)*

The Ku-band of the radio-frequency spectrum offers advantageous properties for observation of snow- and ice-covered areas with imaging radar (Ulaby et al. 1981, King et al. 2015). This can be attributed to a relatively short but non-zero penetration depth, which allows probing of physical characteristics of surface layers through polarimetry. Furthermore, the short wavelength of the Ku-band provides sensitivity to millimeter-scale displacements, which enables estimation and monitoring of glacier flow on short timescales through interferometry. However, most satellite radar sensors operate in other frequency bands, and thus comprehensive datasets observing snow and ice at Ku-band are still relatively rare. Furthermore, radar sensors usually operate in the so-called monostatic observation geometry, where the transmitter and the receiver are placed in the same location. Bistatic capabilities (i.e. placing the transmitter and the receiver in different locations) enable an extension of the observation space and can provide more information, but are not easily accessible.

In this submission we present preliminary results of a radar observation campaign in the Great Aletsch Glacier area. Using KAPRI, a ground-based real-aperture radar sensor with full-polarimetric, interferometric, and bistatic capabilities (Stefko et al., 2022), we monitored the Jungfraufirn area during two seasons (late summer 2021 and late winter 2022), acquiring a comprehensive dataset of monostatic and bistatic observations at Ku-band. The radar dataset is complemented with in-situ examinations of snow cover properties, as well as data from a local meteostation.

Figure 1: Primary KAPRI instrument observing the Jungfraufirn area from the terrace of High Altitude Research Station Jungfraujoch.

This dataset aims to provide insight into changes of the scattering properties of the snow cover over short timescales of the daily cycle, as well as longer, seasonal scales. Information about temporal decorrelation at Ku-band acquired in this campaign can be vital for planning and data evaluation of airborne or spaceborne interferometric radar campaigns with longer temporal baselines. Furthermore, the dataset also aims to serve as a testbed for development and validation of snow parameter inversion methods using bistatic Ku-band radar data.

Preliminary results show a major change in the polarimetric scattering properties of the snow cover between the summer and winter season (Figure 2), which can be linked to changes of the snow morphology. Furthermore, time-series observations show that while during winter the properties remain relatively constant over the course of the day, in summer the melt-freeze cycle causes rapid changes of the polarimetric properties over the course of hours.

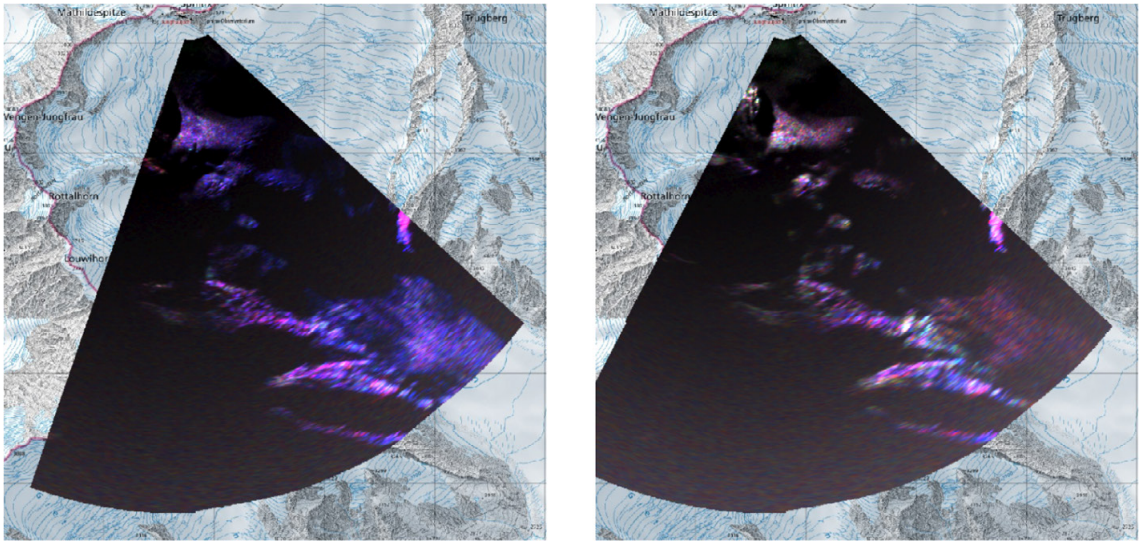

Figure 2. Bistatic polarimetric images of the snow cover acquired in summer (left) and winter (right), shown in the Pauli scattering basis (R: HH-VV, G: HV, B: HH+VV). In summer, dominant blue color indicates the prevalence of surface scattering, suggesting a low penetration depth and presence of melt-freeze crusts. In winter, a more diverse color mix indicates a more disordered medium and higher penetration, resulting in dominance of volume scattering processes.

REFERENCES

King, J., et al. 2015: Spatio-temporal influence of tundra snow properties on Ku-band (17.2 GHz) backscatter, Journal of Glaciology, 61(226), 267-279. doi:10.3189/2015JoG14J020

Stefko, M., et al. 2022: Calibration and Operation of a Bistatic Real-Aperture Polarimetric-Interferometric Ku-Band Radar, IEEE Transactions on Geoscience and Remote Sensing, vol. 60, pp. 1-19, doi: 10.1109/TGRS.2021.3121466.

Ulaby, F. T., et al. 1981: Microwave remote sensing : active and passive. Noorwood (Mass.), Artech House.

19.18
Assessing the 2018 drought response of Swiss forests and its dependence on different hydrological drivers

Joan Sturm[1], Vincent Humphrey[1,2], Maria J. Santos[1], and Alexander Damm[1,3]

[1] Geographisches Institut, University of Zurich, Winterthurerstrasse 190, CH-8057 Zürich (joantracy.sturm@geo.uzh.ch)
[2] Institute for Atmospheric and Climate Science, ETH Zurich, Zürich, Switzerland
[3] Eawag, Swiss Federal Institute of Aquatic Science and Technology, Dübendorf, Switzerland

Consequences of current and projected climate change include the increasing frequency of extreme events. More and stronger drought events, for example, affect health and functioning of forest ecosystems, unsettle related ecosystem services with consequences for economy and human well-being. Thus, understanding the impact of droughts on forest ecosystems is crucial to optimize future forest management strategies.

Quantifying drought impacts on forests requires the understanding and decoupling underlying hydrological drivers. Precipitation is the largest driver of water availability, whereas temperature controlls the atmospheric water demand. The combination of these push and pull processes controll the water transport through the vegetation. Furthermore, tree height and location in forests determine the exposition of individual trees that additionally convolves the meteorological effects of precipitation and temperature. Current climate predictions suggest different trajectories and spatial pattern of precipitation and temperature, which challenges the assessment of drought impacts due to the high variability of the individual hydrological drivers in both space and time.

We present an approach to disentangle the partial impacts of these hydrological drivers, namely water availability, water demand, and exposure, on the response or Swiss forests to the extreme summer drought in 2018. Canopy water content was used as indicator of forest health and was approximated by the Normalised Difference Water Index (NDWI) derived from Sentinel-2 satellite imagery on 10x10 m pixel scale (Sturm et al. 2022). We calculated the potential water availability and combined it with the precipitation anomaly of 2018. The water demand was approximated by the water vapour pressure deficit. Tree exposure was derived from a digital vegetation height model. We then mapped the composition of partial impacts of water availability, demand, and exposure on forest drought responses across Switzerland to see which regions are dominated by one of these drivers. Furthermore, we analysed the strength, direction, and spatial consistency of the driver and impact relationships. Our results provide important insight about the spatial variability of hydrological drivers on forest drought responses and contribute advancing future forest management practices.

REFERENCES

Sturm, J., Santos, M. J., Schmid, B., & Damm, A. (2022). Satellite data reveal differential responses of Swiss forests to unprecedented 2018 drought. Global Change Biology, 28(9), 2956-2978.

P 19.1
Earthquake-volcano interactions at oblique subduction margins; focus on Mount Sinabung volcano (Indonesia)

Benoit Goudard[1], Társilo Girona[2], Luca Caricchi[1], Matteo Lupi[1]

[1] *Department of Earth Sciences, University of Geneva, Genève, Switzerland*
[2] *Geophysical Institute, University of Alaska Fairbanks, Fairbanks, AK, USA*

In 2010 after four centuries of quiescence, Mount Sinabung (Northern Indonesia) erupted and released large amounts of ash and debris forcing thousands of residents to leave their villages. The system develops upon the Great Sumatran Fault, a major strike slip fault accommodating the oblique subduction of the Australian plate beneath the Sunda plate. Mount Sinabung began to inflate approximately 2 years after the occurrence of the Nias earthquake (8.7 Mw), 2005, that struck offshore Sumatra.

Several studies show causal relationships between earthquakes and volcanic eruptions, thus the Nias earthquake could have been responsible for the reawakening of Mount Sinabung in 2010. Here we determine through satellites-measurements the large-scale thermal unrest of Mount Sinabung from several years prior to 2010 until present-day. Radiance emitted by volcano surfaces and measured by MODIS instrument aboard Aqua and Terra satellites is a new method that can be used to analyse the temporal evolution of volcanic activity. We analyse the time evolution of radiance over an area of 20 km x 20 km around Mount Sinabung at 121 locations. We are testing if structural features control the different patterns we observe by correlating the location of major faults, the variations of radiance and the distribution of earthquakes following the Nias event. This new approach is promising as it may allow identifying volcanic unrest years before an eruption and in our case could serve to establish the causal relationships between the Nias earthquake and the 2010 Mount Sinabung eruption.

P 19.2
A fully polarymetric 50 GHz temperature radiometer

Witali Krochin[1,2], Gunter Stober[1,2], Axel Murk[1,2], Roland Albers[1], Tobias Plüss[1]

[1] *Institute of Applied Physics, University of Bern, Sidlerstrasse 5, 3012 Bern (witali.krochin@unibe.ch)*
[2] *Oeschger Centre for Climate Change Research, University of Bern, Hochschulstrasse 4, 3012 Bern*

Continuous temperature measurements in the stratosphere (12-50 km) and the mesosphere (50-80 km) are crucial for the deeper understanding of the physical processes in the middle atmosphere and for the vertical coupling between the different atmospheric layers. Several studies have shown the importance of atmospheric waves such as planetary waves, tides, and gravity waves, their propagation and breaking at these altitudes, and its effect on the global circulation.

Investigating these effects requires long-term measurements with high temporal resolution and altitude coverage. Satellite data covers the required altitude range but provides limited temporal resolution due to its fixed orbital geometry. Active measurement techniques such as LIDAR are usually limited to nighttime and only a few instruments have daytime capability and therefore are unsuitable for continuous observations. Ground-based microwave radiometry provides a robust observational method that is independent of the daytime, almost independent of the weather conditions, and that permits to perform continuous soundings from 20-60 km altitude.

TEMPERA (TEMPErature RAdiometer) is a ground-based radiometer developed at the University of Bern in 2013 (Stähli 2013). It measures microwave radiation spectra from atmospheric oxygen in a range between 52 GHz and 53 GHz. Atmospheric temperature profiles can be retrieved from these spectra. In the last 9 years, the accuracy and performance of this instrument were continuously improved (Krochin 2022). The latest version of TEMPERA has a temporal resolution of one measurement per 30 min and temperature profiles can be retrieved up to an altitude of about 50 km.

The reason for the altitude limitation is the Zeeman effect, which occurs due to the interaction of the atmospheric oxygen with the Earth's magnetic field. The polarization of atmospheric radiation affected by the Zeeman effect depends on the orientation of the propagation direction to the magnetic field. Therefore, the altitude range for temperature retrievals could be further improved by decomposing the measured radiation in its polarization components. In addition, the inclusion of the Zeeman effect in the retrieval algorithm provides the ability to retrieve the Earth's magnetic field from measurements of atmospheric microwave emissions.

The microwave group from the Institute of Applied Physics of the University of Bern, is currently developing a temperature radiometer (TEMPERA-C), which is based on the former instrument (TEMPERA) but allows a fully polarimetric analysis of the atmospheric emission spectra (Krochin 2022). Here we present a simple calibration method and first measurements as well as simulations of atmospheric temperature and magnetic field retrievals from fully polarimetric microwave spectra.

REFERENCES

Krochin, W., & Navas-Guzmán, F., & Kuhl, D., & Murk, A., & Stober, G. 2022: Continuous temperature soundings at the stratosphere and lower mesosphere with a ground-based radiometer considering the zeeman effect, Atmos. Meas. Tech., 15, 2231–2249

Krochin, W., & Stober, G., & Murk, A. 2022: Development of a Polarimetric 50-GHz Spectrometer for Temperature Sounding in the Middle Atmosphere, IEEE Journal of Selected Topics in Applied Earth Observations and Remote Sensing, 15, 5644 – 5651

Stähli, O., & Murk, A., & Kämpfer, N., & Mätzler, C., & Eriksson, P. 2013: Microwave radiometer to retrieve temperature profiles from the surface to the stratopause, Atmos. Meas. Tech., 6, 9, 2477–2494

P 19.3
Quantitative Characterization of Glacier Surging in Karakoram using Synthetci Aperture Radar Data

Shiyi Li[1], Philipp Bernhard[1], Irena Hajnsek[1,2]

[1] *Institute of Environmental Engineering, ETH Zurich, 8093 Zurich, Switzerland* (shiyi.li@ifu.baug.ethz.ch)
[2] *German Aerospace Center (DLR) e.V. Microwaves and Radar Institute, Wessling, Germany*

The Karakoram range in High Mountain Asia (HMA) is well-known for the clustering of surge-type glaciers, which are distinguished by the quasiperiodic flow pattern including a long-lasting quiescent phase and a short-lived active phase. Investigating glacier surges helps to better understand local glacier evolution and to reduce glacier related risks such as glacier lake outburst flood (GLOF). However, the mechanisms of surging in the Karakoram Mountains are not yet fully understood due to the complexity of their dynamics.

In this work, we comprehensively characterized the recent surge of the South Rimo Glacier in Karakoram, which was observed between 2018 and 2020. The South Rimo Glacier represents one of the largest glaciers in the east range of Karakoram. The surge showed combined feature of both thermal and hydrological regulated processes, and thus is a very interesting example for studying surge mechanisms.

To depict the dynamics of the surge, we collected spaceborne Synthetic Aperture Radar (SAR) data from TanDEM-X and Sentinel-1. The main objective is to characterize the changes of the surface elevation, the flow velocity, and the surface thermal regime.

The TanDEM-X COSSC data were acquired between 2011 and 2019 and were used to derive Digital Elevation Models (DEMs). The obtained DEMs were differentiated to calculate the glacier surface elevation changes before and after the surge. The Sentinel-1 images were acquired between 2017-2020 in both ascending and descending orbits. They were adopted to map glacier flow velocities using the offset tracking method. To improve the robustness of offset tracking, we employed the stacked cross-correlation instead of the traditional pair-wise cross-correlation when estimating offsets.

The DEM differencing results showed that the surge front started building-up since 2013. Flow velocity was found gradually increasing starting from 2017, initiating the surge in summer 2018 and reaching the maximum in the mid of 2019. From the Sentinel-2 images, we identified that a supraglacial lake was formed in July 2019 when the surge velocity was maximized. The lake drained in September 2020, and meanwhile the velocity dropped to the pre-surge level.

In our work, inclusive datasets that depict the surge dynamics of the South Rimo Glacier, and quantatitive investigation of the controlling mechanisms of the surge through simulations are presented. It is highlighted that the high spatial-temporal resolution SAR observations provied invaluable information in quantifying glaicer dynamics.

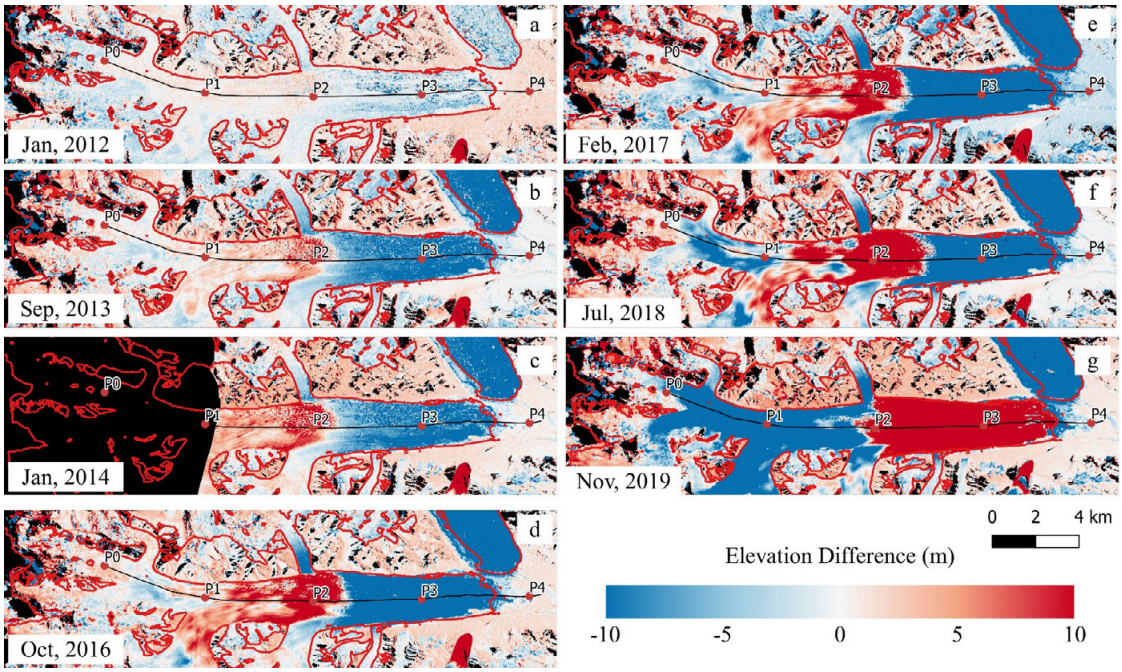

Figure 1. DEM difference maps with respect to 2011-07-15. Reference points P0–P4 roughly divides the manually drawn central flow line into five equal-length parts.

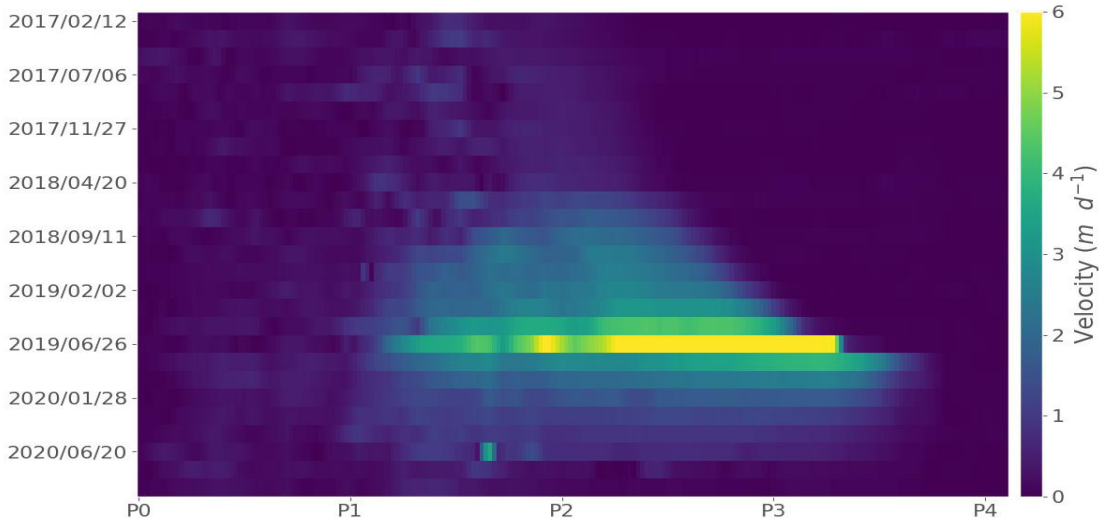

Figure 2. The surface flow velocity of the South Rimo Glacier.

REFERENCES

S. Li, S. Leinss and I. Hajnsek, „Cross-Correlation Stacking for Robust Offset Tracking Using SAR Image Time-Series,“ in IEEE Journal of Selected Topics in Applied Earth Observations and Remote Sensing, vol. 14, pp. 4765-4778, 2021, doi: 10.1109/JSTARS.2021.3072240.

P 19.4
Multi-temporal forest mapping at the Swiss alpine treeline

Thiên-Anh Nguyen[1], Marc Russwurm[1], Benjamin Kellenberger[1,2], Devis Tuia[1]

[1] Environmental Computational science and Earth Observation laboratory, Ecole Polytechnique Fédérale de Lausanne, Rue de l'Industrie 17, CH-1950 Sion (thien-anh.nguyen@epfl.ch)
[2] Center for Biodiversity and Global Change and Department of Ecology and Evolutionary Biology, Yale University, New Haven, CT 06511, USA

The position of the upper alpine treeline is known to be highly sensitive to undergoing climate change. Rising temperatures and their impact on environmental conditions like snow cover shift the position of the treeline upwards in altitude. In the Swiss Alps, land use change (predominantly land abandonment caused by the decline of alpine farming) is also responsible for many of the forest cover changes observed at the treeline ecotone (Gehrig-Fasel et al. 2007). Measurements of treeline responses to such drivers have shown that treeline dynamics are slow and lagged in time. Such insights are traditionally derived from scarce and expensive field measurements, or comparison of coarse historical forest maps. This prevents the creation of multi-temporal and high spatial resolution forest maps spanning several decades, which are needed to better understand the drivers of treeline dynamics in space and across scales. We thus aim at providing high-resolution multi-temporal forest maps at the treeline ecotone over the Valais and Vaud Alps in Switzerland.

We use a collection of geo-referenced aerial images (SwissImage), captured between 1998 and 2017 in various lighting conditions and with various sensors, and downsampled to a common ground resolution of 50 cm. As forest reference and supervision source, we use a forest map derived from the Swiss Topographic Landscape Model (SwissTLM3D), corresponding to the state of the forest around 2017.

We develop a deep learning-based forest mapping method, which predicts a 1 m resolution forest map for each step of a time series of 5 to 9 aerial images. We adapt a mono-temporal forest mapping model (U-net, Ronneberger et al. 2015), pre-trained on the most recent images (2017), to obtain a multi- temporal model — we feed the time series sequentially, and for a given time step, reuse the model output corresponding to the previous time step as an additional input. We train this recurrent model to minimize both a forest segmentation loss applied to the last time step only and a temporal consistency loss, which encourages the output of the model to remain consistent over time.

Results obtained by applying our pre-trained mono-temporal model on the time series show that the pre-trained model can generalize to older images, for those images which are similar enough to the pre-training images (Figure 1). Using the fine-tuned, recurrent model helps aligning detection boundaries for sharp forest edges with no changes, but decreases the performance for the first time steps of the times series, due to the initialization of the recursion loop. This suggests the need for a model integrating more complex temporal components such as GRU (Cho et al. 2014) or LSTM (Hochreiter & Schmidhuber 1997) cells, enabling the model to make use of past predictions in a dynamical way. Future work will thus consist in incorporating such components in our model, while accounting for known forest dynamics at the treeline (slow forest gain, abrupt forest loss).

REFERENCES

Cho, K., Van Merriënboer, B., Gulcehre, C., Bahdanau, D., Bougares, F., Schwenk, H., & Bengio, Y. (2014). Learning phrase representations using RNN encoder-decoder for statistical machine translation. EMNLP 2014 - 2014 Conference on Empirical Methods in Natural Language Processing, Proceedings of the Conference, 1724–1734. https://doi.org/10.3115/v1/d14-1179

Gehrig-Fasel, J., Guisan, A., & Zimmermann, N. E. (2007). Tree line shifts in the Swiss Alps: Climate change or land abandonment? *Journal of Vegetation Science*, *18*(4), 571–582. https://doi.org/10.1111/j.1654-1103.2007.tb02571.x

Hochreiter, S., & Schmidhuber, J. (1997). Long Short-Term Memory. Neural Computation, 9(8), 1735–1780. https://doi.org/10.1162/neco.1997.9.8.1735

Ronneberger, O., Fischer, P., & Brox, T. (2015). U-net: Convolutional networks for biomedical image segmentation. Lecture Notes in Computer Science (Including Subseries Lecture Notes in Artificial Intelligence and Lecture Notes in Bioinformatics), 9351, 234–241. https://doi.org/10.1007/978-3-319-24574-4_28

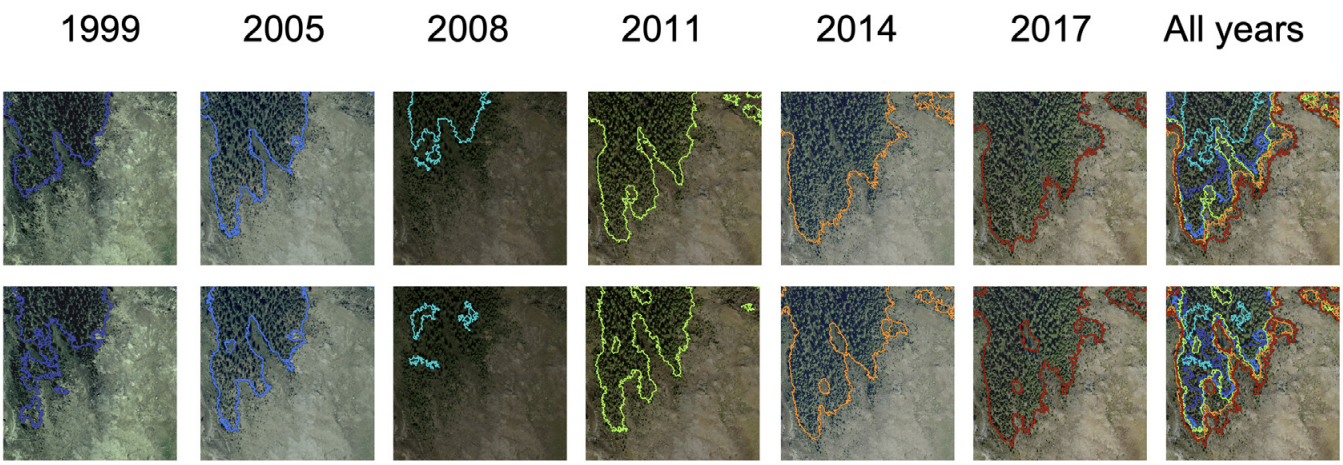

Figure 1. Segmentation boundaries in an alpine area undergoing a gradual treeline shift. Top row: mono-temporal pre-trained model, bottom: fine-tuned recurrent model.

P 19.5
Ozone and Water Vapor Variability in 2019/2020 Arctic Stratospheric Polar Vortex Compared to Climatology

Guochun Shi[1,2], Witali Krochin[1,2], Axel Murk[1,2], Gunter Stober[1,2]

[1] *Institute of Applied Physics, University of Bern, Sidlerstrasse 5, CH-3012 Bern (guochun.shi@unibe.ch)*
[2] *Oeschger Center for Climate Change Research, University of Bern, Hochschulstrasse 4, CH-3012 Bern*

The stratospheric polar vortex in the 2019/2020 winter/spring was the long-lasting, strongest, and coldest on record in the Arctic. Using satellite observations, reanalysis data, and Microwave radiometer measurements we investigate the dynamic structure of the stratospheric polar vortex and relate them to the ozone and water vapor variability. Analyses of ozone and water vapor observations made over Ny-Ålesund indicate that stratospheric ozone was significantly below the climatological average, but mesospheric water vapor is above the climatological average during the stratospheric polar vortex. The polar vortex development to break up in 2019/2020 winter/spring caused unprecedented negative ozone anomalies throughout the winter and extremely high positive water vapor anomalies in mid-spring. High ozone anomalies concentrated along the vortex edge are due to both greater increases in diabatic descent along the vortex and chemical loss in the vortex interior. As a dynamical tracer, water vapor can separate air masses of different properties inside and outside the vortex. Water vapor anomalies across the polar vortex edge in the upper stratosphere and lower mesosphere are high because of the modulation of the polar vortex edge and the advection of extra-vortex air.